

Determination of the transport lifetime limiting scattering rate in InSb/ $\text{Al}_x\text{In}_{1-x}\text{Sb}$ quantum wells using optical surface microscopy

Christopher J. McIndo^{a,*}, David G. Hayes^a, Andreas Papageorgiou^a, Laura A. Hanks^{a,1}, George V. Smith^a, Craig P. Allford^a, Shiyong Zhang^b, Edmund M. Clarke^b, Philip D. Buckle^a

^a School of Physics and Astronomy, Cardiff University, Queen's Buildings, The Parade, Cardiff CF24 3AA, United Kingdom

^b EPSRC National Centre for III-V Technologies, North Campus, University of Sheffield, Sheffield S3 7HQ, United Kingdom

ARTICLE INFO

Keywords:

Magnetotransport
Nomarski microscopy
Electron scattering
Transport lifetime

ABSTRACT

We report magnetotransport measurements of InSb/ $\text{Al}_{1-x}\text{In}_x\text{Sb}$ quantum well structures at low temperature (3 K), with evidence for 3 characteristic regimes of electron carrier density and mobility. We observe characteristic surface structure using differential interference contrast DIC (Nomarski) optical imaging, and through use of image analysis techniques, we are able to extract a representative average grain feature size for this surface structure. From this we deduce a limiting low temperature scattering mechanism not previously incorporated in transport lifetime modelling of this system, with this improved model giving strong agreement with standard low temperature Hall measurements. We have demonstrated that the mobility in such a material is critically limited by quality from the buffer layer growth, as opposed to fundamental material scattering mechanisms. This suggests that the material has immense potential for mobility improvement over that reported to date.

1. Introduction

Indium antimonide (InSb) exhibits the lowest reported electron effective mass ($m^* = 0.014 m_e$) [1] and highest reported room-temperature electron mobility ($\mu_e = 78,000 \text{ cm}^2 \text{ V}^{-1} \text{ s}^{-1}$) [1] of any compound semiconductor. These properties make InSb particularly suited to many electronic applications including low power high frequency electronics and quantum device realisation. There has been a recent resurgence of interest in the development of high quality InSb material following the report of two-dimensional electron gas (2DEG) channel mobilities in excess of $200,000 \text{ cm}^2 \text{ V}^{-1} \text{ s}^{-1}$ at $T = 1.8 \text{ K}$ [2–5], and the possibility of Majorana fermion observation in InSb nanowires [6,7].

Furthermore, the strong spin-orbit interaction and extremely large Landé g -factor ($g \approx -50$) [1,8] exhibited in InSb has gained attention for potential exploitation in spintronics and quantum information control [9–11].

Previous studies of carrier transport in InSb 2DEGs [3,4] have considered standard scattering mechanisms using the relaxation time approximation and described the mobility variation over a wide range of temperature (typically 3–293 K). Whilst there has been good agreement, parameters used have tended to be extreme values to

enable acceptable fits to data. It is believed that a major scattering mechanism associated with material quality has not been considered previously, with this having a major effect on the mobility behaviour. Considering this additional structural scattering allows for far more reasonable values for standard scattering mechanisms, showing that there is immense potential for mobility improvement in this material.

2. Growth and sample details

The InSb quantum well heterostructures studied were grown by solid source molecular beam epitaxy (MBE) on semi-insulating GaAs substrates (and so are therefore lattice mismatched with regard to the substrate). In growth order, the epitaxy comprises an aluminium antimonide (AlSb) accommodation layer, a $3 \mu\text{m} \text{ Al}_{0.1}\text{In}_{0.9}\text{Sb}$ strain-relieving barrier layer (to allow for mismatch relaxation), a 30 nm InSb quantum well layer and a 50 nm $\text{Al}_{0.15}\text{In}_{0.85}\text{Sb}$ top barrier layer. Tellurium (Te) δ -doping is introduced into the top barrier, 25 nm above the InSb quantum well (QW). Deliberate doping of the lower barrier is avoided in order to prevent any impurity donor atoms being carried forward on the growth plane which could significantly compromise the transport lifetime of carriers in the quantum well. Hall bar devices with an aspect ratio of 5:1 (nominally $200 \mu\text{m} \times 40 \mu\text{m}$) were

* Corresponding author.

E-mail address: mcindocj@cardiff.ac.uk (C.J. McIndo).

¹ Present address: Physics Department, Lancaster University, Lancaster LA1 4YB, United Kingdom.

fabricated using standard photolithography, mesa wet etching and metal evaporation techniques. Relatively low temperature fabrication processes were used ($\leq 100^\circ\text{C}$) to prevent excess metal penetration and tellurium dopant migration in the samples. The fabricated devices were mounted into non-magnetic ceramic leadless chip carriers and contact between the package and devices made via gold fine wire wedge bonding.

3. Experimental determination of mobility and sheet carrier density

All samples were measured over a range of temperature between 2.8 K and 300 K using a closed cycle pulse tube cryostat. The sample, when placed in the cryostat, was situated between the poles of a 0.6 T electromagnet. Electrical measurements of the samples were performed using a combination of a Keithley 6221 Current Source Meter and a Keithley 2401 Nanovoltmeter, using a pseudo-AC technique to remove any voltage drifts due to heating. To determine the mobility and carrier density, a constant current of either $1\ \mu\text{A}$ or $2\ \mu\text{A}$ was applied and the resulting transverse and longitudinal voltages recorded. No heating effects were observed with use of different current values. The magnetic field was then swept from 0 T to 0.6 T and from 0 T to $-0.6\ \text{T}$, and this was repeated as a function of temperature.

Fig. 1(a) shows the measured longitudinal (R_{xx}) and transverse Hall resistance (R_{xy}) for a typical sample at temperatures of 3 K, 50 K and 150 K. Also shown are 2 carrier fits to the data [12], with the fits matching well to the data. The fitting gives a 2D sheet carrier density (n_{2D}) of $\sim 3 \times 10^{11}\ \text{cm}^{-2}$ and mobility $\sim 200,000\ \text{cm}^2\ \text{V}^{-1}\ \text{s}^{-1}$, with n_{2D} increasing slightly over the temperature range studied.

Fig. 1(b) shows the extracted mobilities and carrier densities for a range of different samples at 3 K. Samples with increasing δ -doping (filled symbols) broadly define three regimes in the data. Initially, in

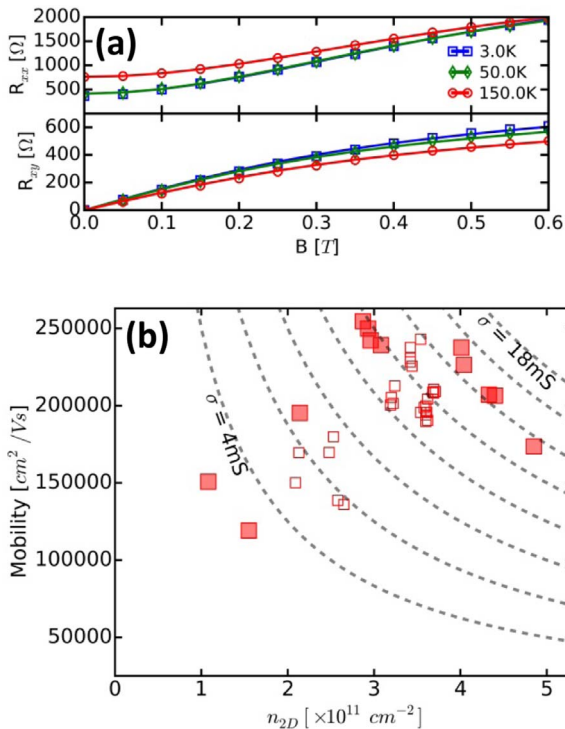


Fig. 1. (a) Typical longitudinal (R_{xx}) and Hall (R_{xy}) resistance vs. B -field for 3 K, 50 K and 150 K (symbols, every 25th data point plotted for clarity) with 2 carrier fits shown as solid lines [12]. (b) Measured mobility (two carrier fit) vs. 2D sheet carrier density (n_{2D}) from 3 K Hall measurements. A series of samples with increasing δ -doping levels is shown by the larger, filled symbols, showing at first an increasing mobility with carrier density. This then plateaus before then decreasing. Smaller, unfilled symbols indicate samples from other growth batches. Dashed lines are contours of constant conductance.

region 1, an increasing mobility is observed for an increase in carrier concentration n_{2D} (from $1 \times 10^{11}\ \text{cm}^{-2}$ to $3 \times 10^{11}\ \text{cm}^{-2}$). This is believed to be due to single subband filling, calculated from Schrödinger-Poisson (S.P.) modelling [13], giving rise to increased Thomas-Fermi screening. The mobility, μ , then begins to plateau at $\sim 250,000\ \text{cm}^2\ \text{V}^{-1}\ \text{s}^{-1}$ for a narrow range of carrier densities (region 2), before decreasing beyond $4 \times 10^{11}\ \text{cm}^{-2}$ (region 3). In region 3, Schrödinger-Poisson modelling shows there is the possibility of multiple subband occupancy and additional intersubband scattering.

4. Nomarski image analysis

To help examine the limiting factors affecting the higher mobility samples, the surface morphology was considered using optical differential interference contrast DIC (Nomarski) imaging. To analyse the material surface multiple microscope images were taken of various samples in a spread of positions on the surface. Images were taken at an optical magnification of $\times 50$. A raw Nomarski image of a standard wafer with $n_{2D} \sim 3 \times 10^{11}\ \text{cm}^{-2}$ and $\mu \sim 200,000\ \text{cm}^2\ \text{V}^{-1}\ \text{s}^{-1}$ is shown in Fig. 2.

The Nomarski image shows clear surface roughness, present similarly on all wafers imaged in this study. The roughness consists of approximately circular features with clear boundaries separating features. Due to the proximity of the 2DEG to the surface, it is reasonable to assume that this surface roughness, and in particular the boundaries, have a severe impact on the electron transport in the quantum well active layer.

Multiple grey scale images were taken of each wafer, and for each image, a small square sub-image was extracted using a window typically 200 pixels by 200 pixels of the original image. This ensured each sub-image contained many features. The sub-image was kernel smoothed to remove noise from the image and a 2D polynomial was fitted to remove any background trend (blush) in the image. To calculate the number of features, a 2D gradient was calculated by first determining gradients in the x and y directions, and depending on illumination, calculating the sum of or difference in these gradients. Any region above a set threshold was labelled as a definable feature and subsequently counted, giving the total number of features for the sub image. This analysis was repeated for multiple windows on each image (typically 40 sub images), with results combined to give a mean feature count, the error given by the standard deviation. This process was repeated for all images of each wafer, and corresponding feature counts averaged with errors combined in quadrature.

To turn the feature count into an average feature size, it was assumed that the features filled all space, and therefore the average area of each feature was given by the area of the sub-image divided by the mean feature count. A comparison of the mean feature diameter calculated using this Nomarski imaging analysis to the mean free paths, λ , deduced from a basic Drude transport model, is shown in Fig. 2. The mean free paths are calculated using mobilities from standard 3 K Hall measurements of samples shown in Fig. 1, as well as from historical samples from references [3,4,14,15].

There is a clear trend in measured mean free path with mobility, reaching a peak mean free path of $\sim 2.5\ \mu\text{m}$. Fig. 2 shows the calculated feature diameter is approximately constant across all samples measured, with a mean value of $\sim 2.43 \pm 0.13\ \mu\text{m}$. This is in excellent agreement with the maximum mean free path deduced from mobility measurement, and is strongly suggestive that at low temperatures, when phonon effects are reduced, an electron traveling in the quantum well may travel ballistically through a feature until it reaches a boundary, causing a scattering event and ultimately limiting the transport lifetime. It is speculated therefore that the surface features are the low temperature limiting scattering mechanism in determining high electron mobilities in the QW. Further advancement in mobility and mean free path without significant buffer redesign will be impossible.

Download English Version:

<https://daneshyari.com/en/article/5449976>

Download Persian Version:

<https://daneshyari.com/article/5449976>

[Daneshyari.com](https://daneshyari.com)